Modeling the Maximum Specific Absorption Rate in the Human Eye

***Li Liu*[1], *Natalia K. Nikolova*[2]**

[1]Department of Electrical and Computer Engineering, McMaster University, Hamilton, ON, L8S 4K1, Canada, liul33@mcmaster.ca

[2]Department of Electrical and Computer Engineering, McMaster University, Hamilton, ON, L8S 4K1, Canada, talia@mcmaster.ca

Abstract

We present a fast semi-analytical model to predict the maximum specific absorption rate (SAR) in the eye under the influence of antennas whose open-space near-field pattern is known. The model is verified by comparison with full-wave simulations, which include the antenna and the eye immersed in a head-equivalent medium. Several antennas are investigated, such as a dipole, a loop, a patch and a printed inverted-F antenna (PIFA). We show that resonance effects occur in the eye at the frequencies used in wireless communications and these effects may cause local SAR values to exceed exposure limits.

1. Introduction

Equipment which utilizes or emits electromagnetic (EM) energy may be hazardous through uncontrolled and excessive emissions [1]. Thermal effects due to radio-frequency (RF) or microwave energy can be a serious health hazard especially to the human eye [2]. Regulatory bodies have set exposure limits in terms of the specific absorption rate (SAR) [3, 4]. In the case of the eye, the limit for the average SAR over 10 grams of tissue is 2 W/kg in the frequency range from 0.5 to 3.5 GHz. Some of these frequencies are used in wireless services.

There is increased demand for the current third-generation (3G) and the future 4G mobile phones to be capable of video phone or high-speed interactive-internet data formats. Under these formats, when the unit is in a full-duplex (transmit and receive at same time) operation, the hazard to the human eye is of significant concern. This is because the handheld unit is usually placed close to the eyes for prolonged periods while the unit may transmit at full power.

It is known that SAR measurements and testing pose a serious challenge to the wireless industry, the government regulators, and to researchers. In some studies, SAR values were extrapolated from the temperature changes measured by implanted thermal probes [5]. However, this technique is not suitable for regular testing in industrial and government laboratories. Most estimations of the whole-body SAR value are performed using Dewar flask or twin-well calorimetry [6]. Such liquid phantoms can lead at best to average estimates of SAR over large volumes of tissues. However, they lack the complexity and the detail inherent to biological structures.

Here, we present a new method for fast maximum SAR evaluation in the human eye due to handheld devices. In Section 2, we discuss the resonance effects in the human eye at the frequencies used by the wireless services. We present a simplified analytical model of the resonant modes. Section 3 outlines our semi-analytical model which predicts the value of the maximum SAR as a function of the antenna orientation and the antenna input power when the antenna free-space near-field pattern is known.

2. Simplified Analytical Model

Our investigations show that the electric field distribution in the human eye can be adequately modelled using a simplified geometry. In this simplified geometry, the eyeball is a sphere-shaped vitreous body which constitutes more than 90% of the eyeball volume [7]. The host medium in which the eyeball is immersed is the weighted average of tissues such as skin, fat, brain and bone [7]. We refer to this medium as the bio-medium. The complex permittivity and the conductivity of eye tissues can be found in [8]. Fig. 1 shows the geometry of this simplified model together with the parameters of the eyeball and the bio-medium.

Due to the high permittivity contrast between the eye sphere and the bio-medium, the sphere has distinct resonant modes. These modes are the solutions to the Helmholtz equations for the **E** and **H** field solved in terms of spherical functions. The resonant frequencies are obtained from the eigenvalue equations for the TE and the TM modes [7, 9]:

a) TE_{nmp} modes

$$\frac{I_{n+1/2}(\gamma_1 a)}{\gamma_1 I_{n-1/2}(\gamma_1 a)} = \frac{K_{n+1/2}(\gamma_2 a)}{\gamma_2 K_{n-1/2}(\gamma_2 a)} \tag{1}$$

b) TM_{nmp} modes

$$\frac{\gamma_1}{j\omega\tilde{\varepsilon}_1}\frac{I_{n-1/2}(\gamma_1 a)}{I_{n+1/2}(\gamma_1 a)} - \frac{n}{j\omega\tilde{\varepsilon}_1 a} = \frac{\gamma_2}{j\omega\tilde{\varepsilon}_2}\frac{K_{n-1/2}(\gamma_2 a)}{K_{n+1/2}(\gamma_2 a)} - \frac{n}{j\omega\tilde{\varepsilon}_2 a} \tag{2}$$

Here, I and K are the modified Bessel functions [10]. The eigenvalue equations are obtained by imposing the conditions of field continuity at the interface between the eye sphere and the bio-medium. In (1) and (2), the radius of the eyeball a is 1.3 cm, $\tilde{\varepsilon}_{1,2} = \varepsilon_{1,2} - j\sigma_{1,2}/\omega$ and $\gamma_{1,2} = j\omega(\mu\tilde{\varepsilon}_{1,2})^{1/2}$. The equations are solved for ω, which yields an infinite discrete spectrum of resonant frequencies. Table I shows the resonant frequencies of the dominant modes of the eyeball resonator. We note that these resonant frequencies are close to those used in modern cellular services.

Once the resonant frequency is known, we obtain the field distribution for a mode. For the TM_{101} mode, at the resonant frequency of 0.9 GHz, we have

$$E_r = \frac{2}{r^2}\hat{I}_1(\gamma_1 r)\cdot\cos\theta\sqrt{2}, \qquad E_\theta = \frac{1}{r}\left(\gamma_1\hat{I}_0(\gamma_1 r) - \frac{1}{r}\hat{I}_1(\gamma_1 r)\right)\cdot\sin\theta, \qquad E_\phi = 0 \tag{3}$$

We verify the simplified analytical model of the resonant effects in the eye sphere through HFSS simulations [11]. We adopt the same geometry as in Fig. 1 and a plane-wave excitation. Fig. 2 shows the normalized field distribution along the axis of the eye. The analytical curve corresponds to the dominant TM_{101} field in (3). The result of the simulation confirms the existence of this resonant mode and its dominant role in determining the field distribution. Note that the field has its maximum in the center of the eye which is typical for the dominant TM_{101} mode. It is obvious that the resonance in the eye has a low quality factor Q, which is due to the high loss. This simple analytical model and the HFSS simulations predict that the maximum of the field distribution and, therefore, of the maximum SAR are located in the middle of the eyeball. The distribution of the next TE_{101} mode is similar.

3 Prediction of Maximum SAR

An important parameter of our analytical resonance model is the ratio R_{mb} of the maximum field-magnitude value $|E_{\max}|$ occurring in the center of the eye and its boundary value $|E_b|$ at the surface of the eye. Once we have this ratio, we can set $|E_b|$ equal to an effective boundary value of the electric field calculated from the near field of the antenna and we can obtain $|E_{\max}|$ as well as the highest SAR value $\mathrm{SAR}_{\max}$.

To calculate the equivalent boundary value of the field E_b, we apply weighted averaging of the near field at 6 points located symmetrically on the surface of the eyeball resonator. The field complex values $E_{\zeta i}$, $\zeta = r, \theta$, $i \in [1,6]$, are taken from the open-space near-field data of the antenna. The weighting coefficient depends on the distance D_i, $i \in [1,6]$, between the ith point and the center of the eye:

$$c_i = D_i / \sum_{i=1}^{6} D_i \tag{4}$$

The weighting coefficients are shown in Table II in the case of a distance D = 20 mm and eye radius a = 1.3 cm. We define R_{mb} as

$$R_{mb} = |E_{\max}| / |E_b|, \tag{5}$$

$$E_b = \sum_{i=1}^{6} c_i E_i. \tag{6}$$

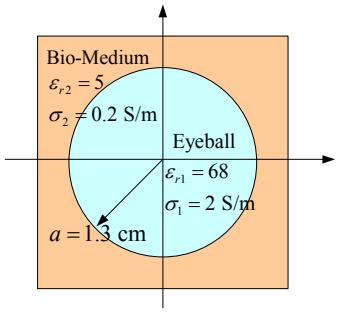

Fig. 1. The geometry of the simplified analytical model.

TABLE I
The Resonant Frequencies of the Analytical Model

Mode	TM_{101}	TE_{101}	TM_{201}	TE_{201}	TE_{202}
f_r (GHz)	0.9	1.8	2.4	2.8	3.2

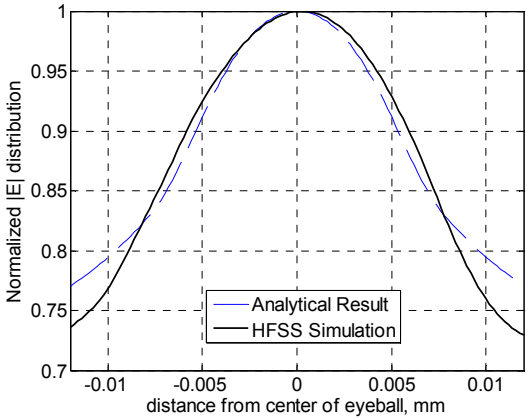

Fig. 2. The electric field distribution along the eye's axis obtained from the simplified analytical model and the HFSS simulation ($a = 1.3$ cm, $f = 0.9$ GHz).

To verify the ability of our semi-analytical model to predict R_{mb}, we compare its output with a detailed simulation model. It includes the vitreous body, a skin layer with a circular aperture in front of the eye, a region of fat and layers of bone and brain [7]. We investigate different antennas such as a small loop, a small dipole, a large loop, a right-hand circularly polarized patch and a printed inverted-F antenna (PIFA) [12]. The dimensions of each antenna are listed in Table III. The distance from each antenna to the surface of the eyeball is 20 mm.

The results for R_{mb} obtained from the semi-analytical model and the simulation are summarized in Table IV. Here, the maximum error refers to the case of excitation where disagreement is the largest. Overall, the maximum error between the semi-analytical model and the simulation model is less than 15%. Therefore, the semi-analytical model can adequately predict the ratio of the maximum to boundary field value and predict the maximum SAR value from $|E_b|$.

In summary, our algorithm for maximum SAR evaluation consists of the following steps: 1) calculating the resonant frequencies of the eyeball depending on its size; 2) calculating the ratio R_{mb} of the maximum to boundary field value at each resonant frequency from (3), see also Fig. 2; 3) calculating the equivalent boundary value of the field on the eyeball surface $|E_b|$ from the near-field data using (6); 4) calculating the maximum field $|E_{\max}|$ from (5); and 5) calculating the maximum SAR using $\mathrm{SAR}_{\max} = \sigma |E_{\max}|^2 / \rho_m$, where σ is the conductivity of the vitreous body and ρ_m is its mass density.

4. Conclusion

We have presented a fast semi-analytical model which predicts quickly and reliably the maximum SAR in the human eye. The agreement with detailed and time-consuming EM simulations is better than 15%. The model requires the near-field data of the antenna, which can be obtained either by simulation or by measurement in open space.

Furthermore, we find that the human eye acts as a resonator at the frequencies used for wireless services regardless of the mutual position and orientation of the antenna and the eye. In the present study, we chose the antennas to be only 20 mm from the eye. This is a worst-case or even an impractical scenario; however, it is an example at which the maximum SAR in the eye may easily exceed the limit of 2 W/kg.

The resonance of the eye in the wireless frequency range has been ignored in the derivation of the current SAR limits and the respective testing procedures. These need to be revisited. Further studies are needed to include the effects of thermal exchange and blood flow. Experimental work is planned for the development of eye phantoms and novel testing procedures.

TABLE II
Weighted Coefficients for $|E_b|$ (D=20 mm, a=1.3 cm)

Point	1	2	3	4	5	6
Coeff.	0.28	0.08	0.16	0.16	0.16	0.16

TABLE III
Antenna Size

Antenna	**Size**
small dipole	length: 26.5 mm
small loop	radius: 0.4 mm
large loop	radius: 4.5 mm
RHCP patch	length of patch: 8 mm length of substrate: 11.25 mm
PIFA	length: 2 mm; Width: 1.8 mm

TABLE IV
R_{mb} Ratios

The worst case		**Resonant Frequencies (GHz)**			
		0.9	1.8	2.8	3.2
analytical model		1.23	1.61	2.56	1.98
simulations with different antennas	plane wave	1.17	1.55	2.49	1.90
	small dipole	1.24	1.55	2.61	1.85
	small loop	1.15	1.48	2.76	1.87
	large loop	1.26	1.75	2.38	1.87
	RHCP patch	1.29	1.75	2.60	1.99
	PIFA	1.21	1.52	2.19	1.96
maximum error (%)		4.8	8.1	14.4	6.6

5. References

1. A. V. Vorst, A. Rosen, and Y. Kotsuka, *RF/Microwave Integration with Biological Tissues*, New York: J. Wiley & Sons, 2005.

2. S. Lönn, A. Ahlborn, P. Hall, and M. Feychting, "Long-term mobile phone use and brain tumor risk," *American Journal of Epidemiology*, 2005, vol. 161, no. 6, pp. 526-535.

3. IEEE Std C95.1™-2005, "IEEE standard for safety levels with respect to human exposure to radio frequency electromagnetic fields, 3 kHz to 300 GHz," New York, 2005.

4. ICNIRP, "Guideliens for limiting exposure to time-varying electric, magnetic, and electromagnetic fields (up to 300 GHz)," *Health Physics*, 1988, pp. 494-522.

5. C. H. Durney, H. Massoudi, and M. F. Iskander, *Radiofrequecy Radiation Dosimetry Handbook*, Brooks: School Aerospace Med. of USAF, 1986.

6. J. P. Padilla, *Using Dewar-Flask Calorimetry and Rectal Temperatures to Determine the Specific Absorption Rates of Small Rodents*, Brooks: School Aerospace Med. of USAF, 1986.

7. L. Liu, "A Study of the Specific Absorption Rate in the Human Eye," *Tech. Report of CEM Lab. McMaster Univ.*, May 2007, vol. 40.

8. D. L. Means, and K. W. Chan, *Evaluating Compliance with FCC Guidelines for Human Exposure to Radiofrequency Electromagnetic Fields*, Washington D. C.: Federal Communications Commission, 2001.

9. M. Gastine, L. Courtois, and J. L. Dormann, "Electromagnetic resonances of free dielectric spheres," *IEEE Trans. Microwave Theory & Tech.*, 1967, vol. 15, no. 12, pp. 694-700.

10. C. A. Balanis, *Advanced Engineering Electromagnetics*. New York: J. Wiley & Sons, 1938.

11. Ansoft HFSS ver. 10.1.2, Ansoft Corporation, 225 West Station Square Drive, Suite 200, Pittsburgh, PA 15219, USA, 2006, www.ansoft.com.

12. M. F. Abedin, and M.Ali, "Modifying the ground plane and its effect on planar inverted-F antennas (PIFAs) for mobile phone handsets," *IEEE Antennas and Wireless Propagation Letters*, 2003, vol. 2, pp. 226-229.